Available online at www.sciencedirect.com
SCIENCE DIRECT®
Materials Research Bulletin 39 (2004) 1557–1567
Materials Research Bulletin
www.elsevier.com/locate/matresbu

Hydrothermal synthesis, characterization and magnetic properties of $NaVGe_2O_6$ and $LiVGe_2O_6$ ☆

Mehtap Emirdag-Eanes[a,*], Joseph W. Kolis[b]

[a]*Department of Chemistry, Faculty of Science, Izmir Institute of Technology, Gulbahce koyu, Urla, Izmir 35430, Turkey*
[b]*Department of Chemistry, Clemson University, Hunter Research Lab., Clemson, SC 29634-0973, USA*

Received 16 July 2003; received in revised form 16 July 2003; accepted 2 April 2004

Abstract

Supercritical fluids are shown to be an excellent reaction media for the synthesis of novel solid state phases at intermediate temperatures. $LiVGe_2O_6$ and $NaVGe_2O_6$ have the common pyroxene structure composed of VO_6 linear chains. $NaVGe_2O_6$ crystallizes in the monoclinic space group $C2/c$ with four formula units having cell dimensions $a = 9.960(4)$ Å, $b = 8.853(10)$ Å, $c = 5.4861(10)$ Å, $\beta = 106.403(3)^\circ$. The structure was refined until $R = 0.0290$ and $R_w = 0.0370$. For $LiVGe_2O_6$ in space group $P2_1/c$: $a = 9.8508(7)$ Å, $b = 8.754(3)$ Å, $c = 5.3948(13)$ Å, $\beta = 108(3)^\circ$, $R = 0.0240$ and $R_w = 0.0250$. The compounds contain edge-shared VO_6 octahedral chains and corner-shared GeO_4 tetrahedral chains. The presence of these VO_6 chains results in spin-Peierls distortion. Structural and physical characterization of the compounds are reported.

Keywords: A. Inorganic compounds; D. Crystal structure; D. Magnetic properties; C. X-ray diffraction

1. Introduction

Vanadium oxides have a fascinating chemistry because of their variation in oxidation states and coordination geometry, where one can find octahedral, square pyramidal, tetrahedral as well as trigonal bipyramidal environments. Vanadium metal can have several oxidation states in its compounds, which allow them to have very interesting optical, magnetic and catalytic properties. The common oxidation states of vanadium in solid state compounds are +3, +4 and +5. Trivalent vanadium has two d-electrons, which are responsible for some unusual magnetic and optical properties.

☆ Supplementary data associated with this article can be found, in the online version, at doi:10.1016/j.materresbull.2004.04.001.

* Corresponding author. Tel.: +90 232 498 7564; fax: +90 232 498 7509.
E-mail address: mehtapemirdag@iyte.edu.tr (M. Emirdag-Eanes).

0025-5408/$ – see front matter
doi:10.1016/j.materresbull.2004.04.001

$LiVGe_2O_6$ has recently been synthesized as a powder and its magnetic properties were studied by Millet et al. [1]. This system is clearly a spin-1 chain, but its magnetic susceptibility is very different from other spin-1 chains, which is probably due to a spin-Peierls phase [2,3]. After successfully synthesizing some well-formed crystals of rare earth germanates, we attempted to synthesize some new vanadium phases, which could have unusual properties.

The title compounds, $LiVGe_2O_6$ and $NaVGe_2O_6$, take on the pyroxene structure, which will accept a wide variety of metals [4–6]. Alkali metal pyroxenes are extremely attractive due to the variety of cations. For $A^+M^{3+}Si_2O_6$, A = Li, Na and M can be Al, Ga, In, or certain transition metals such as Fe^{3+}, Cr^{3+}, Mn^{3+}, Ti^{3+}, Sc^{3+} and V^{3+} [7]. $LiVSi_2O_6$ [8], $LiAlSi_2O_6$ [9], $LiFeSi_2O_6$ [9], $LiScSi_2O_6$ [10], $LiInSi_2O_6$ [11] and $LiGaSi_2O_6$ [12] are the only known lithium members of these types of compounds to date. The silicate form is more common than the germanate, but there are a few known $AMGe_2O_6$ compounds in the literature such as $NaFeGe_2O_6$ [13]. Many scientists have studied variations in the different pyroxenes [8–12]. Their studies have shown that Li and Na pyroxenes have the same type of structure with the space group *C*2/*c*. This structure type has one-dimensional edge-sharing VO_6 chains, which are responsible for interesting magnetic properties such as the spin-Peierls transition, especially when vanadium (III or IV) ions are present. Vanadium (III) has two d-electrons, which allows it to form a spin-1 chain and vanadium (IV) has one d-electron that allows it to form a spin-1/2 chain.

2. Experimental section

2.1. General

Qualitative elemental analysis on single crystal samples of the title compounds were obtained by energy dispersive spectrometry (EDS) using a JEOL JSM-IC 848 scanning microscope equipped with a Princeton Gamma Tech (PGT) PRISM detector, which indicated the presence of Na, V, Ge and O with no significant impurity heavier than F. Optical absorption spectra were obtained on a PC-controlled SHIMADZU UV-3100 UV–vis/near-IR spectrometer equipped with an integrating sphere. $BaSO_4$ was used as the reflectance standard. After the sample was crushed on filter paper, absorption spectra were obtained from 200 to 2500 nm. Data was collected in reflectance (*R*%) mode and manually converted to absorbance (α/s) from the relationship, $A = \alpha/s = (1 - R\%)2/2R\%$ commonly called the Kubelka–Munk function [14], where α is the absorption coefficient and s is the scattering coefficient. Band gaps were refined by extrapolating the linear portion of the absorption edge to $(\alpha/s)^{1/2} = 0$ where $h\nu \approx E_g$. The linear portion of the absorbance edge versus energy (eV) spectra was chosen, and $(\text{absorbance})^2$ and $(\text{absorbance})^{1/2}$ were calculated, and separately plotted as a function of eV. These two curves were subjected to a linear curve fit and the plot having the greatest linearity represented the nature of the optical band gap [15]. The magnetic susceptibility of crystalline compounds were measured by a Quantum Design SQUID (super conducting quantum interference device) MPMS-XE magnetometer. Relatively clean single crystals (2–20 mg) were manually selected, placed into the top of a gel cup. The measurements were typically carried out from 2 to 300 K in a field of $H = 0.5$–1 T and the change in the total magnetization versus temperature was measured at each temperature. The magnetic susceptibility was corrected for the container and for the core diamagnetism. Temperature dependence of the magnetic susceptibility of a single crystal of $NaVGe_2O_6$ (1.1 mm × 0.2 mm × 0.2 mm, and

0.044 mg) was performed from 2 to 300 K, under a magnetic field strength of 5 T parallel to each of the three crystal axes.

2.2. Synthesis

Single crystals of the title compounds were synthesized from 0.015 g (1×10^{-4} mol) V_2O_3 and 0.042 g (4×10^{-4} mol) GeO_2. NaOH (1.05 M) was used to synthesize the $NaVGe_2O_6$. The starting materials were added to the 0.25 cm OD silver tubes followed by 0.4 mL NaOH and then the tubes were welded shut. These tubes were then placed into a Tuttle "cold sealed" autoclave and heated at 580 °C for 3 days. Dark green crystals of $NaVGe_2O_6$ were obtained with 100% yield. Similarly, LiOH (0.5 M) was used as a solvent mineralizer and the reactions were heated at 591 °C for 3 days to yield $LiVGe_2O_6$ (60%, light green needles) and 40% Li_2VGeO_5 purple polyhedral crystals. Li_2VGeO_5 will be the subject of a future paper.

2.3. Structure determination

A crystal of $NaVGe_2O_6$ with the approximate dimensions of 0.15 mm × 0.07 mm × 0.07 mm and 0.3 mm × 0.3 mm × 0.3 mm for $LiVGe_2O_6$ was mounted on a glass fiber with epoxy glue and centered on the four-circle Rigaku AFC8 diffractometer equipped with a Mercury CCD array detector. Data were collected at room temperature (~300 K) using graphite monochromated Mo Kα ($\lambda = 0.71073$ Å) radiation.

The unit cell parameters and the orientation matrix were initially determined from a set of seven screening frames taken at equal intervals of 30° in ω using a 1D Fourier algorithm [16]. Reflection indexing, Lorentz-polarization correction, peak integration and background determination were performed using the *CrystalClear* software. A box size of 15 × 15 pixels (each pixel corresponds to about 140 μm) was used for the integration of all reflections. Unit cell parameters were refined after integration using all observed reflections to yield the following values: $a = 9.960(4)$ Å, $b = 8.853(10)$ Å, $c = 5.4861(10)$ Å, $\alpha = 90°$, $\beta = 106.403(3)°$ and $\gamma = 90°$ for $NaVGe_2O_6$ and $a = 9.8508(7)$ Å, $b = 8.754(3)$ Å, $c = 5.3948(13)$ Å, $\alpha = 90°$, $\beta = 108(3)°$ and $\gamma = 90°$ for $LiVGe_2O_6$.

An empirical absorption correction was applied using a REQABA routine in the *CrystalClear* software package. The structure was solved by direct methods SIR-92 and refined on F by full matrix, least squares techniques with TEXSAN [17] and SHELXTL-PLUS [18]. All atomic thermal parameters were refined anisotropically. Crystallographic data are given in Table 1, and atomic coordinates, equivalent isotropic displacement coefficients are given in Table 2.

3. Result and discussion

$LiVGe_2O_6$ and $NaVGe_2O_6$ have similar structures although they have different space groups, $P2_1/c$ and $C2/c$, respectively. The unit cell views of both compounds are given down the c-axis in Fig. 1, and the similarities are very interesting. We have tried to solve the structure of both compounds in the same space group $C2/c$, which is a common space group for pyroxene compounds. However, we were unable to solve the structure of $LiVGe_2O_6$ in $C2/c$ successfully. X-ray powder patterns of the compounds did not match, suggesting different structure types. $NaVGe_2O_6$ is C-centered, because reflections of the type hkl with $h + k = 2n + 1$ are systematically absent. The reason for the different lattice types could

Table 1
Crystal data and structure refinement for $LiVGe_2O_6$ and $NaVGe_2O_6$

Empirical formula	$LiVGe_2O_6$	$NaVGe_2O_6$
Crystal system, space group	Monoclinic, $P2_1/c$	Monoclinic, $C2/c$
Unit cell dimensions		
a (Å)	9.627(2)	9.960(4)
b (Å)	8.754(3)	8.853(6)
c (Å)	5.395(1)	5.486(1)
β (°)	108.35(13)	106.103(3)
Volume (Å^3), Z	441.5(2), 4	461.1(3), 4
Formula weight	299.06	315.11
Density (calculated) (mg/m^3)	4.498	4.510
Absorption coefficient (cm^{-1})	15.535	14.879
Temperature (K)	293.2	300.2
2θ range (°)	6.38–59.60	6.26–59.66
Index ranges	$-12 \le h \le 11$, $-11 \le k \le 11$, $-7 \le l \le 6$	$-13 \le h \le 12$, $-12 \le k \le 11$, $-7 \le l \le 6$
Total reflectance/independent reflectance	4627/1128	2440/623
Observed reflections	718 ($I > 3.0\sigma(I)$)	517 ($I > 3.0\sigma(I)$)
Number of parameters	92	48
Weighting scheme	$w^{-1} = \sigma^2(F) + 0.0003F^2$	
Final R indices (observed data)	$R = 2.40\%$, $wR = 2.50\%$	$R = 2.90\%$, $wR = 3.70\%$
Goodness-of-fit	1.28	1.42
Largest different peak and hole (e Å^{-3})	0.81, −0.71	1.26, −1.35

Table 2
Atomic coordinates ($\times 10^4$) and equivalent isotropic thermal parameters of compounds

Atom	x	y	z	U_{eq}
$NaVGe_2O_6$				
Ge1	0.21132(3)	1.09549(4)	0.26727(6)	0.00546(12)
V1	0.0000	0.40824(9)	0.2500	0.0051(2)
Na1	0.0000	0.8055(3)	0.2500	0.0140(5)
O1	0.3932(2)	1.0829(3)	0.3655(5)	0.0061(5)
O2	0.1393(2)	1.0154(3)	0.4938(4)	0.0106(6)
O3	0.1385(2)	1.2711(3)	0.1851(5)	0.0097(6)
$LiVGe_2O_6$				
Ge1	−1.05270(5)	0.65920(8)	−0.81890(8)	0.00538(13)
Ge2	−1.45395(5)	0.65720(8)	−1.23631(8)	0.00572(13)
V3	−1.24848(9)	0.34304(11)	−0.96117(13)	0.0045(2)
O4	−1.3831(4)	0.4788(5)	−1.1711(7)	0.0129(10)
O5	−0.8648(4)	0.6674(5)	−0.7519(6)	0.0074(9)
O6	−1.3592(4)	0.1672(5)	−1.1769(6)	0.0059(8)
O7	−1.1314(4)	0.4954(5)	−0.7430(6)	0.0076(9)
O8	−1.3839(4)	0.7106(5)	−1.4963(6)	0.0108(9)
O9	−1.1122(4)	0.8099(5)	−0.6516(6)	0.0099(9)
Li10	−1.2429(11)	0.5155(12)	−0.459(2)	0.015(2)

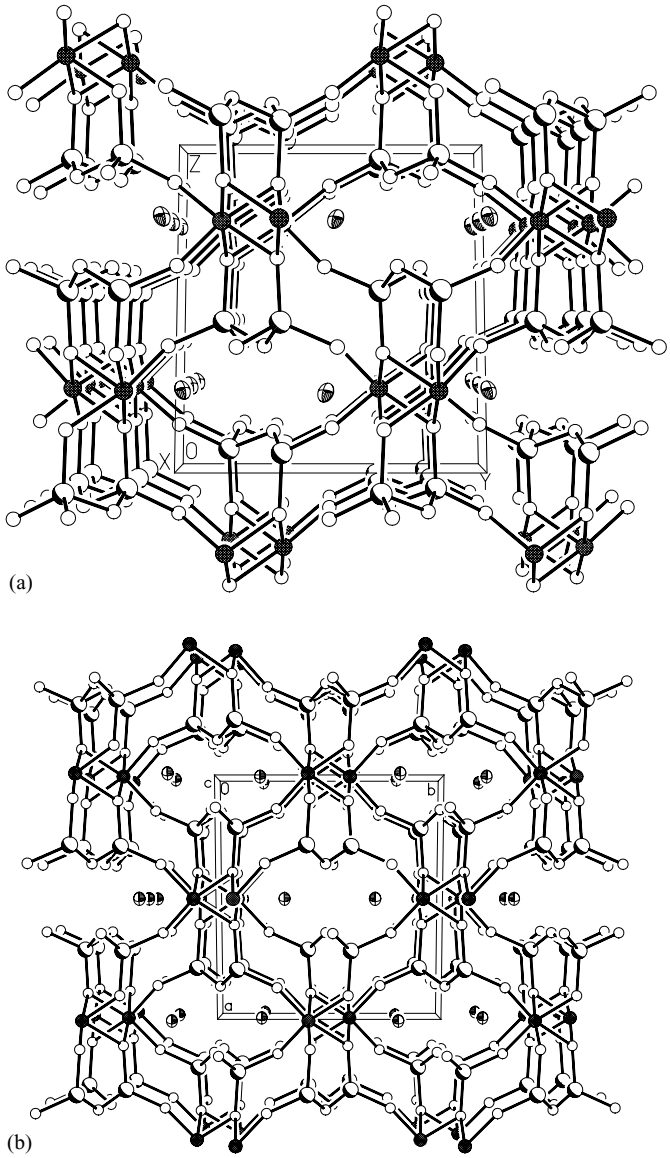

Fig. 1. Unit cell view of (a) $NaVGe_2O_6$ down the *c*-axis, (b) $LiVGe_2O_6$ down the *c*-axis where Ge atoms are shaded circles, V atoms are solid circles, O atoms are open circles and cations are full thermal ellipsoids with 70% probability.

possibly be explained by the differences in cation size. $LiVGe_2O_6$ is definitely not C-centered because there is no systematic extinction among *hkl* reflections. Both structures have systematic extinctions for the two-fold screw axis and *c*-glide; therefore, this did not help to decide the space group. It seemed reasonable to assign the space group of $P2_1/c$ to $LiVGe_2O_6$ because $LiFeGe_2O_6$, $LiAlGe_2O_6$ and $LiGaGe_2O_6$ all have the space group of $P2_1/c$ [19].

It can be seen from the unit cell view of $NaVGe_2O_6$ (Fig. 1a) that vanadium has six bonds to six oxygen atoms, thus forming an octahedron. These VO_6 octahedra are edge shared along the *c*-axis

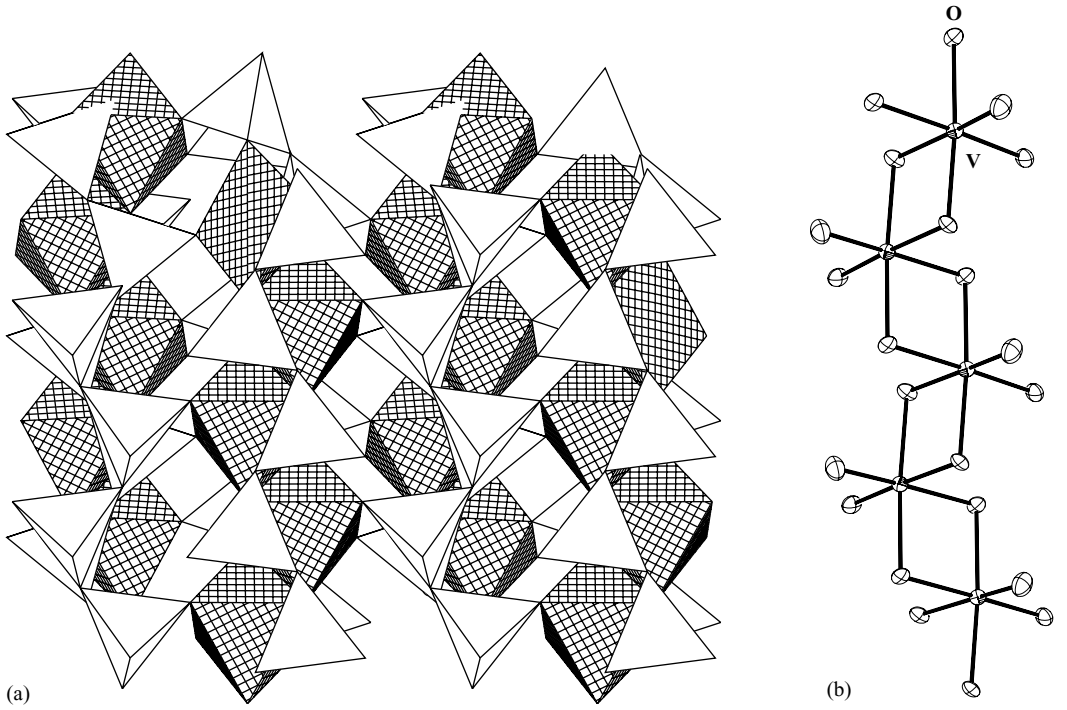

Fig. 2. (a) A polyhedra projection of the unit cell. VO_6 are shown as cross-hatched polyhedra, and GeO_4 tetrahedra are open polyhedra. (b) VO_6 chain in $LiVGe_6O_6$ and $NaVGe_2O_6$.

forming V_2O_{10} dimers that are vertex shared with the GeO_4 tetrahedra. This linkage of octahedra and tetrahedra forms channels along the *c*-axis in which the cations reside. The polyhedra structure for the unit cell of $NaVGe_2O_6$ along the *c*-axis is shown in Fig. 2. Bond distances and angles are basically the same for both compounds (Tables 3 and 4). The average V–O bond distance in VO_6 octahedra is

Table 3
Selected bond distances of compounds (Å)

$NaVGe_2O_6$			
V(1)–O(3)	1.932(3)	V(1)–O(3)	2.062(3)
V(1)–O(3)	1.932(3)	Ge(2)–O(3)	1.715(3)
V(1)–O(1)	2.062(3)	Ge(2)–O(1)	1.735(3)
V(1)–O(1)	2.062(3)	Ge(2)–O(2)	1.736(3)
V(1)–O(1)	2.063(3)	Ge(2)–O(2)	1.755(3)
$LiVGe_2O_6$			
Ge(1)–O(4)	1.760(4)	Ge(2)–O(9)	1.748(5)
Ge(1)–O(7)	1.716(4)	V(3)–O(6)	1.917(5)
Ge(1)–O(8)	1.769(4)	V(3)–O(4)	2.068(5)
Ge(1)–O(8)	1.770(4)	V(3)–O(4)	2.097(4)
Ge(2)–O(6)	1.707(5)	V(3)–O(5)	2.066(5)
Ge(2)–O(4)	1.749(4)	V(3)–O(5)	2.068(3)
Ge(2)–O(9)	1.758(4)	V(3)–O(7)	1.950(5)

Table 4
Selected bond angles (°) of compounds

$NaVGe_2O_6$			
O(3)–V(1)–O(3)	102.64(17)	O(3)–V(1)–O(1)	91.61(11)
O(3)–V(1)–O(1)	166.54(12)	O(1)–V(1)–O(1)	79.95(12)
O(3)–V(1)–O(1)	87.75(11)	O(1)–V(1)–O(1)	96.77(11)
O(3)–V(1)–O(1)	87.75(11)	O(1)–V(1)–O(1)	175.66(14)
O(1)–V(1)–O(1)	166.54(12)	O(3)–Ge(2)–O(1)	117.62(13)
O(3)–V(1)–O(1)	83.39(15)	O(3)–Ge(2)–O(2)	108.91(13)
O(3)–V(1)–O(1)	91.61(11)	O(1)–Ge(2)–O(2)	110.77(13)
O(1)–V(1)–O(1)	91.10(12)	O(3)–Ge(2)–O(2)	103.99(14)
O(1)–V(1)–O(1)	96.77(11)	O(1)–Ge(2)–O(2)	111.48(12)
O(3)–V(1)–O(1)	79.95(12)	O(2)–Ge(2)–O(2)	102.89(9)
O(3)–V(1)–O(1)	91.10(12)		
$LiVGe_2O_6$			
O(4)–Ge(1)–O(7)	118.4(2)	O(6)–Ge(2)–O(5)	115.8(2)
O(4)–Ge(1)–O(8)	107.9(2)	O(6)–Ge(2)–O(9)	101.4(2)
O(4)–Ge(1)–O(8)	105.7(2)	O(6)–Ge(2)–O(9)	112.9(2)
O(7)–Ge(1)–O(8)	106.7(2)	O(5)–Ge(2)–O(9)	109.8(2)
O(7)–Ge(1)–O(8)	108.4(2)	O(5)–Ge(2)–O(9)	110.8(2)
O(8)–Ge(1)–O(8)	109.7(2)	O(9)–Ge(2)–O(9)	105.2(2)
O(6)–V(3)–O(4)	169.1(2)	O(4)–V(3)–O(7)	91.2(2)
O(6)–V(3)–O(4)	89.3(2)	O(4)–V(3)–O(4)	80.9(2)
O(6)–V(3)–O(5)	86.8(2)	O(4)–V(3)–O(4)	175.0(2)
O(6)–V(3)–O(5)	94.0(2)	O(4)–V(3)–O(7)	98.5(2)
O(6)–V(3)–O(7)	98.3(2)	O(5)–V(3)–O(4)	95.6(2)
O(4)–V(3)–O(4)	94.6(2)	O(5)–V(3)–O(7)	174.9(2)
O(4)–V(3)–O(4)	83.8(2)	O(5)–V(3)–O(7)	84.7(2)
O(4)–V(3)–O(5)	81.5(2)		

2.03(8) Å, while the average Ge–O bond distance in GeO_4 is 1.75(2) Å (Table 3). This V–O bond length is in agreement with the study of Schindler et al. [20]. Their study shows that the distribution of V^{3+}–O bond lengths has a range of 1.88–2.18 Å. The VO_6 octahedron is distorted with an average O–V–O right angle of 90(5)° and GeO_4 is a distorted tetrahedra with an O–Ge–O angle of 109(5)°. The environment of the cation in the two compounds is different. The Li ion has five bonds to oxygen atoms with average bond distances of 2.16(9) Å. However, in the sodium analog, the sodium atom has six bonds to oxygen with an average bond distance of 2.46(4) Å.

4. Physical properties

4.1. Diffuse reflectance measurements

Both compounds absorb strongly at wavelengths around 450 nm and 700 nm. Light of wavelengths between 500 and 700 nm is almost completely transmitted. This result correlates with the color of the crystals. The calculated optical band gap is 2.4 eV (510 nm) for $LiVGe_2O_6$ and 2.3 eV (534 nm) for $NaVGe_2O_6$.

4.2. Magnetic measurements

As previously stated, VO_6 octahedra are edge shared down the *c*-axis to form V_2O_{10} dimers, which are vertex shared with GeO_4 tetrahedra. This linkage of octahedra results in a very interesting magnetic property called spin-Peierls transition [2,21]. The spin-Peierls transition is one of the most interesting phenomena observed in a low dimensional quantum spin system. It occurs in crystals containing linear 1D chains of spin-1/2 ions coupled by the antiferromagnetic exchange interaction. Below a spin-Peierls transition temperature, T_{sp}, the structure underlying the lattice changes so that the chains become dimerized. The spin-Peierls is a special case of alternating antiferromagnetic chains, whereby the

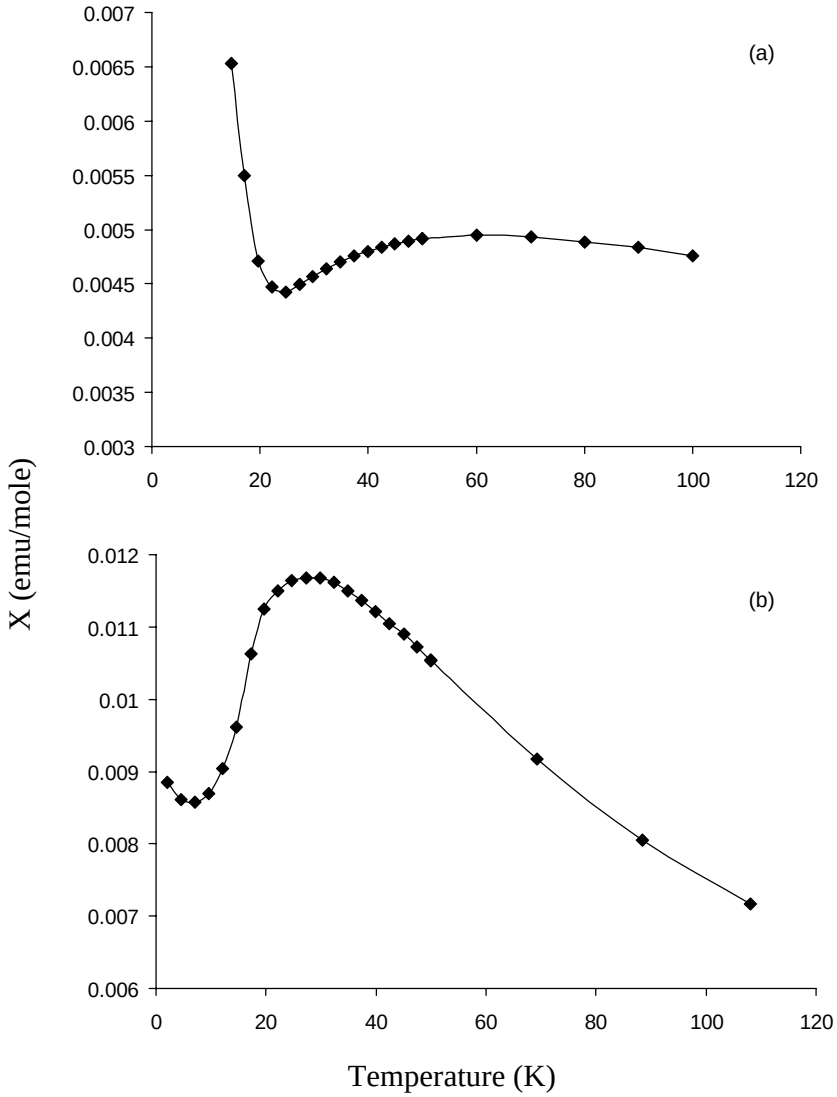

Fig. 3. Plot of magnetic susceptibility: (a) $LiVGe_2O_6$, (b) $NaVGe_2O_6$.

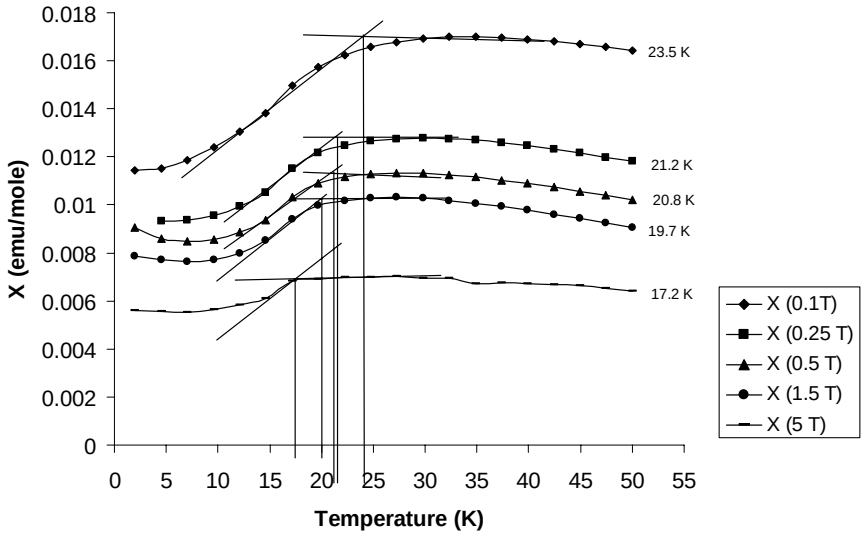

Fig. 4. Field dependence study for $NaVGe_2O_6$.

structure changes by dimerizing because of coupling of magnetic spins rather than electrons. The temperature dependence of the magnetic susceptibility for $NaVGe_2O_6$ is shown in Fig. 3.

Magnetic susceptibility measurements were made by using 1.78×10^{-5} mol of $NaVGe_2O_6$ crystals between 2 and 300 K in a magnetic field of 0.5 T using a SQUID magnetometer. We were also able to perform single crystal measurements and a field dependence study to prove that $NaVGe_2O_6$ has a spin-Peierls transition. It should be noted that $LiVGe_2O_6$ has already been widely established as a spin-Peierls compound [1]. However, this sodium analog is new.

The first requirement for a spin-Peierls transition is that the compound should have a 1D linear chain (Fig. 2b). The second is that susceptibility of the compound should show a rapid decrease below the transition temperature since the spin-Peierls transition is essentially an antiferromagnetic transition. A plot of χ versus temperature is given in Fig. 3 and a very sharp drop was observed in the case of $NaVGe_2O_6$ around 27 K, where the lowest point of the drop occurs at 7 K. There are two possibilities for this drop in magnetic susceptibility. One could explain this as a simple, structural phase change that is occurring as a result of a spin-Peierls transition. In Fig. 4, the temperature dependence of magnetic susceptibility for a crystalline sample of $NaVGe_2O_6$ is shown under various magnetic fields. It can be seen that the transition temperature shifts to lower temperatures with increasing magnetic field, which coincides with a third criterion for spin-Peierl transitions. If it were a simple structural phase transition there would not be a shift of the transition at lower temperatures. Therefore, this field dependence result suggests a spin-Peierls transition. The fourth criterion is that susceptibility in all directions χ_i ($i = a$, b, c) exponentially drops to small, constant values below the transition temperature. This is a very important result. The origin of this rapid decrease in the susceptibility could be due to 3D antiferromagnetic long-range order (AF LRO) or 1D long-like antiferromagnetism [2]. In both cases, the susceptibility decreases rapidly as the temperature approaches 0 K in only one direction of the crystal and remains finite in the other directions. As seen in Fig. 5, there is a decrease of susceptibility in all directions suggesting neither 3D AF LRO, nor 1D long-like antiferromagnetism behavior is taking place.

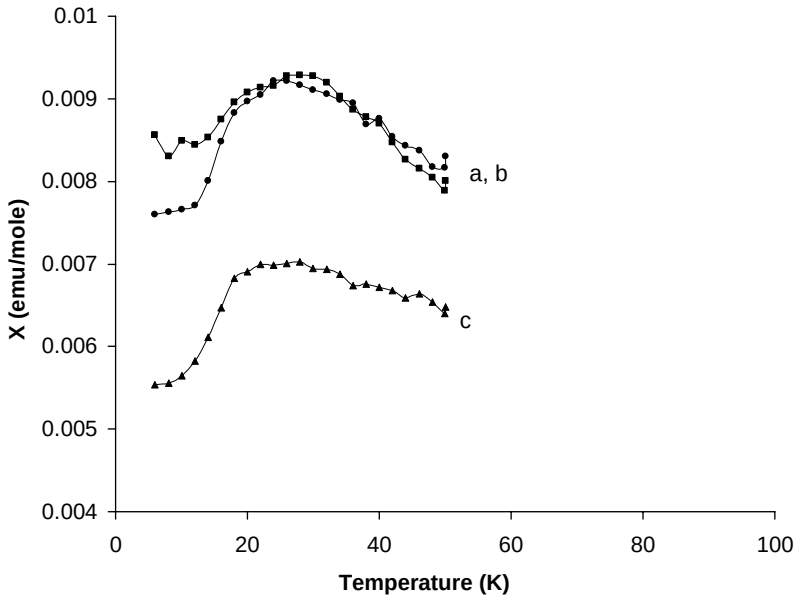

Fig. 5. Temperature dependence of magnetic susceptibility in all directions for $NaVGe_2O_6$.

Acknowledgements

We are indebted to the NSF for support of this work (CHE-9714408). We would also like to acknowledge the NSF (CHE-9808165) for purchase of the CCD diffractometer, and to thank Mutlu Ulutagay for the magnetic measurements.

References

[1] P. Millet, F. Mila, F.-C. Zhang, M. Mambrini, A.B. Van Oosten, V.A. Pashchenko, A. Sulpice, A. Stepanov, Phys. Rev. Lett. 83 (1999) 4176.
[2] J.-P. Renard, L.-P. Regnault, M. Verdaguer, J. Phys. (Paris) 49 (C8) (1988) 1424.
[3] K. Katsumata, J. Magn. Magn. Mater. 140–144 (1995) 1595.
[4] M. Cameron, S. Sueno, C.T. Prewitt, J.J. Papike, Am. Mineral. 58 (1973) 594.
[5] C.T. Prewitt, C.W. Burnham, Am. Mineral. 51 (1966) 956.
[6] F.C. Hawthorne, H.D. Grundy, Acta Crystallogr. B30 (1974) 1882.
[7] H. Ohashi, T. Osawa, K. Tsukimura, Acta Crystallogr. C43 (1987) 605.
[8] C. Satto, P. Millet, J. Galy, Acta Crystallogr. C53 (1997) 1725.
[9] J.R. Clark, D.E. Appleman, J.J. Papike, Miner. Soc. Am. Spec. Pap. 2 (1969) 31.
[10] F.C. Hawthorne, H.D. Grundy, Can. Mineral. 15 (1977) 50.
[11] M. Grotepass, M. Behruzi, T. Hahn, Z. Kristallogr. 162 (1983) 90.
[12] A. Sato, T. Osawa, H. Ohashi, Acta Crystallogr. C50 (1994) 487.
[13] L.P. Salov'eva, V.V. Bakakin, Z. Kristallogr. 12 (1967) 591.
[14] W.W. Wendlandt, H.G. Hecht, Reflectance Spectroscopy, Interscience Publishers, New York, 1966.
[15] J.I. Pankove, Optical Process in Semiconductors, Prentice Hall, Inc., Englewood Cliffs, NJ, 1971.
[16] I. Steller, R. Bolotovsky, M.G. Rossmann, J. Appl. Crystallogr. 30 (1997) 1036.

[17] TEXSAN: Single Crystal Structure Analyses Software, Version 1.6b, Molecular Structure Corporation, The Woodlands, TX 77381, 1993.
[18] G.M. Sheldrick, SHELXTL PLUS, Siemens Analytical X-Ray Instruments, Inc., Madison, WI 53719.
[19] M. Behruzi, Th. Hahn, Fortschr. Mineral. 53 (1) (1975) 4.
[20] M. Schindler, F.C. Hawthorne, W.H. Baur, Chem. Mater. 12 (2000) 1248.
[21] F.D.M. Haldene, Phys. Lett. 93A (1983) 464;
F.D.M. Haldene, Phys. Rev. Lett. 50 (1983) 1153.